

Size determination of free metal clusters by core-level photoemission from different initial charge states

S. Peredkov* and S. L. Sorensen

Department of Synchrotron Radiation Research, Lund University, Box-118, SE-22100, Lund, Sweden

A. Rosso, G. Öhrwall, M. Lundwall, T. Rander, A. Lindblad, H. Bergersen, W. Pokapanich, S. Svensson, and O. Björneholm
Department of Physics, Uppsala University, Box 530, SE-75121, Uppsala, Sweden

N. Mårtensson

Max-lab, Lund University, Box 118, SE-22100, Lund, Sweden

and Department of Physics, Uppsala University, Box 530, SE-75121, Uppsala, Sweden

M. Tchapyguine

Max-lab, Lund University, Box 118, SE-22100, Lund, Sweden

(Received 11 July 2007; published 9 August 2007)

We present the study of free nanoscale lead clusters using photoelectron spectroscopy and synchrotron radiation. Pb 5*d* core-level spectra reveal the presence of different initial charge states of the clusters created by the magnetron-based source. We suggest a method for determining the cluster size from the charge-dependent core level binding energies. Both the core-level and the valence spectra demonstrate that we have created free metallic clusters with essentially the same electronic structure as the solid.

DOI: [10.1103/PhysRevB.76.081402](https://doi.org/10.1103/PhysRevB.76.081402)

PACS number(s): 61.46.Bc, 36.40.-c, 73.30.+y, 79.60.-i

The properties of clusters are to a large extent defined by their finite size. The electronic structure changes drastically with cluster size, from localized atomic levels over molecularlike orbitals for small clusters to bandlike states for large clusters approaching the solid. In metal clusters the filled and unoccupied levels merge at a certain size leading to the emergence of metallicity.¹⁻³

Significant experimental and theoretical efforts have been put into studying geometric and electronic properties of supported metal clusters,^{2,4,5} and of clusters in a free beam.^{3,6} In contrast to supported particles free clusters have an important advantage: there is no cluster-substrate interaction changing the cluster properties.

The optimal method of study would provide information on both the cluster electronic structure and on the size. Photoelectron spectroscopy is a method that maps the electronic structure of the system.^{3,6,7} Until recently for free *metal* clusters only the *valence* band could be probed with this method. *Core-level* photoelectron spectroscopy (XPS) experiments on dilute cluster beams have for a long time been unfeasible due to insufficient sample density for existing x-ray sources. Only with the advent of modern synchrotron facilities could XPS studies of free clusters be performed, primarily for rare gas and molecular clusters created by adiabatic expansion sources.⁸⁻¹²

Photoelectron spectroscopy has no detection limitations imposed by cluster size, in contrast to mass spectrometry.¹³ For nanoscale clusters size determination, a crucial issue in the free cluster studies, becomes challenging for mass spectroscopy. While for the clusters produced by adiabatic expansion the size can be estimated using the Γ^* -formalism¹⁴ there is no such method for large metal clusters created by gas aggregation. Core-level photoelectron spectroscopy is a method where the size is reflected in the bulk-to-surface re-

sponse ratio,^{8,15} and in the absolute binding energy shifts,⁷ but both of these size estimation approaches are limited.

In this Rapid Communication we present a core-level photoelectron spectroscopy study of free metal clusters created with a magnetron-based gas aggregation source. Such a source, in which the magnetron sputtering process vaporizes the solid target into a liquid-nitrogen-cooled cryostat filled with inert gas, is known to be a unique tool for production of clusters from higher melting point materials.^{16,17} We have chosen to study lead, for which the sputtering rate and 5*d* core level ionization cross section are high. The XPS spectral analysis reveals the presence of clusters in various initial charge states in the cluster beam with the *neutral* clusters dominating. Simple modeling of the binding energies for clusters of different charge states permits the determination of cluster size.

The experiments were performed at the soft x-ray undulator beamline I411 at the MAX-lab synchrotron radiation facility (Lund, Sweden).¹⁸ The experimental setup was similar to that used in our previous measurements on a free metal atomic beam and free sodium clusters.^{7,19} Lead vapor was created as the result of the magnetron-discharge-based sputtering process and subsequently clustered in collisions with the cold carrier gas atoms (Ar) in the gas aggregation volume.¹⁹ The carrier gas flow transferred the metal clusters through a narrow nozzle from the cryostat into the experimental chamber, where they were irradiated by the synchrotron light. In contrast to the setup described in Ref. 19 the present experiments were performed without a skimmer and without differential pumping. Emitted photoelectrons were detected by a Scienta R4000 electrostatic electron energy analyzer fixed at 90° to the horizontal polarization plane of the synchrotron radiation. The total experimental energy resolution was in the 120–160 meV range.

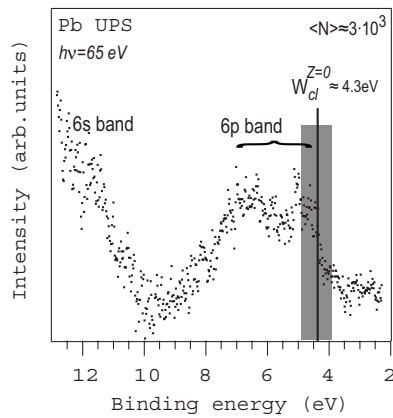


FIG. 1. Valence photoemission spectrum of lead clusters with $\langle N \rangle \approx 3 \times 10^3$ recorded at a photon energy of 65 eV. The binding energy scale is referred to as the vacuum level. The work function of the neutral lead clusters $W_{cl}^{Z=0} \approx 4.3$ eV is shown with a solid line. The gray bar illustrates the range containing the work functions for $Z = +1, 0, -1$ clusters.

Metallic properties of clusters can be disclosed by valence photoelectron spectroscopy, which reflects the density of states (DOS) of the sample, augmented by cross-section effects. Figure 1 presents a typical valence spectrum obtained by sampling the cluster-containing beam. The spectral shape of the recorded features resembles to a great extent the published density of states for solid lead.^{20,21} The feature between 4 and 8 eV arises from bands derived from 6p levels. The similarity between cluster and bulk spectra bears witness to the well-formed metallic properties in lead clusters and thus for the large cluster size. It also means that the concentration of impurities and lead compounds in the cluster beam is low enough to exclude them as the explanation of the additional features in the XPS discussed below.

Since the clusters are produced in the magnetron plasma region, neutral as well as positively and negatively charged clusters are formed.¹⁶ However, the large DOS-related spectral width obscures the information on different charge states of large clusters, for which the DOS does not change significantly with an extra charge.²²

In the earlier reported experiments with free metal clusters created by a magnetron-based source either only positively or only negatively charged clusters were studied.^{17,23,24} Thus the overall pattern of cluster charge-state abundance and especially information on the initially neutral clusters are lost. As will be seen, in our XPS experiment we obtain the entire picture with charge-state resolution.

In the present XPS measurements on large free lead clusters we expected to obtain a spectral pattern similar to that reported for solid Pb (Refs. 25–27) and Pb clusters deposited on a conducting substrate.⁵ This expectation is based on previous studies of metal clusters created by our gas aggregation source.⁷ In order to compare cluster XPS spectra with the solid-state spectra the work function must be taken into account. Indeed the solid XPS energy is referred to the Fermi level, and the free cluster binding energy is measured relative to the vacuum level. The solid lead 5d spectrum contains two well-resolved $5d_{5/2}$ and $5d_{3/2}$ spin-orbit components in the

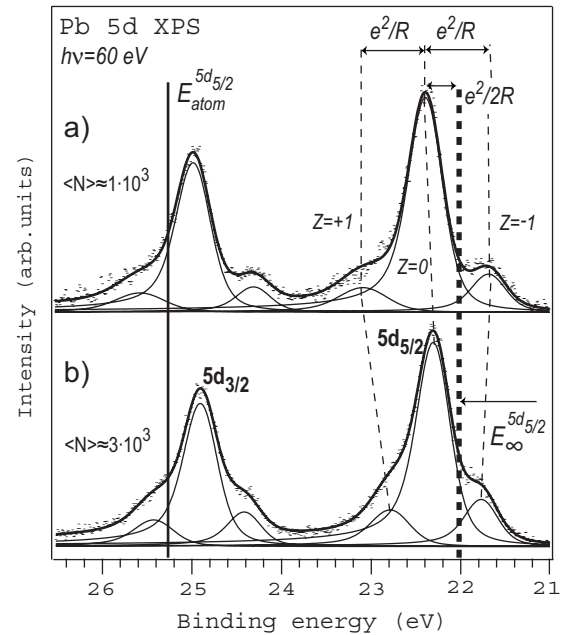


FIG. 2. 5d XPS spectra of lead clusters recorded at a photon energy of 60 eV (dots) for two different clustering conditions: (a) $\langle N \rangle \approx 1 \times 10^3$ and (b) $\langle N \rangle \approx 3 \times 10^3$. The spectra are fitted (solid lines) using Doniach-Sunjić profiles. The lifetime width of 0.2 eV and singularity index $\alpha = 0.1$ are taken similar to the bulk Pb parameters from Ref. 27. In each of the $5d_{5/2}$ and $5d_{3/2}$ spin-orbit related groups the central peak is due to initially neutral ($Z=0$) clusters. Initially positively charged ($Z=+1$) and negatively charged ($Z=-1$) cluster peaks appear symmetrically around the neutral peak.

vicinity of 22 and 25 eV (relative to the vacuum level) separated by ≈ 2.6 eV.^{25,27} Each of these features is the result of overlapping surface and bulk components, for which the binding energy difference is only 0.16 eV.²⁷ Such a small separation is indistinguishable within the inherent peak widths.

In Fig. 2 two photoelectron spectra of the cluster-containing beam recorded in the 5d binding energy region under different clustering conditions are shown. The lower spectrum in Fig. 2(b) was obtained at the same conditions as the valence band spectrum in Fig. 1. The spectrum in Fig. 2(a) was recorded under conditions producing smaller clusters (lower argon pressure). Two groups of similar features around 22.5 and 25.0 eV are obviously related to the $5d_{5/2}$ and $5d_{3/2}$ states. In each group three subcomponents are clearly distinguishable, where the central peak is several times more intense than the other two. The energy separation between the two central peaks in each spin-orbit related group is ≈ 2.6 eV, and the intensity ratio between them is close to the statistical value of 2/3—in agreement with the solid Pb XPS.²⁷ However, further, detailed assignment, namely the explanation of the subcomponents in each group, is at first glance not obvious.

The absence of impurities in the valence region spectrum excludes lead compounds as the source of the extra spectral features. A discrete pattern in the core-level binding energy spectrum due to the size effect can also be excluded. In the

regime of nanoscale cluster production, a magnetron-based source creates a *continuous* size distribution of the clusters, with a single maximum.²⁴ In this size regime, a scaling law is expected to apply, giving a monotonous dependence of the binding energy on size, and therefore the size distribution will not cause a multipeak electron energy spectrum. The width of the feature will, however, be affected by the size distribution. Surface and bulk responses separated by 0.16 eV cannot explain the 0.5 eV [Fig. 2(b)] separation between the subcomponents. Additionally the relative intensity between the subcomponents did not change with photon energy, as would be the case if the components were connected to surface and bulk. Crystal-field splitting can also be ruled out as such a splitting has not been observed in solid lead. Moreover, due to different degeneracies for the $5d_{5/2}$ and $5d_{3/2}$ components a splitting by electric field would lead to a different spectral appearance for each spin-orbit split component.

The magnetron-based gas aggregation source creates from 20% up to 80% charged particles in the beam depending on the magnetron power and carrier gas pressure.¹⁶ In the recorded spectra we expect a signal from initially neutral ($Z=0$) clusters, and from initially positively ($Z=+1$) and negatively ($Z=-1$) charged clusters. Clusters with higher charge states are less likely to be created due to electrostatic considerations. The present experiments were performed at low magnetron power (100 W) which according to Ref. 16 favors neutral cluster production.

A large metal cluster can be approximated by a conducting sphere,²⁸ so that the cluster work function differs from the planar solid work function by a term defined largely by classical electrostatics, and depends on the cluster charge and size. The dependence of the binding energy of the states at the Fermi level $E_{Fermi}(R)$ on the charge state of metal clusters has been recently studied experimentally.²³ In our recent studies of neutral sodium clusters we have shown that the conducting sphere model can also be applied to core-level ionization of metal clusters.⁷ For a given radius R of a conducting cluster its ionization energy $E_{cl}(Z,R)$ is described by the following formula:

$$E_{cl}(Z,R) = E_{\infty} + \Delta E(Z,R) = E_{\infty} + \left(Z + \frac{1}{2}\right) \frac{e^2}{R}, \quad (1)$$

where E_{∞} is the binding energy of the infinite planar bulk relative to the vacuum level, and Z is the initial cluster charge. Thus the core-electron binding energy will be $E_{\infty} + \frac{1}{2} \frac{e^2}{R}$, $E_{\infty} - \frac{1}{2} \frac{e^2}{R}$, and $E_{\infty} + \frac{3}{2} \frac{e^2}{R}$ for initially neutral, singly charged negative and positive clusters, respectively. For clusters of a given size every integral variation in charge changes the binding energy by $\pm \frac{e^2}{R}$.

We have performed fitting of the spectral profile assuming the same shape for all subcomponents. Such an approach resulted in an equidistant separation between the central peak and the side peaks for both spectra in Fig. 2. We found a separation of 0.71 ± 0.02 eV in the upper spectrum (conditions for smaller clusters) and 0.52 ± 0.02 eV in the lower spectrum (conditions for larger clusters). From all above

considerations, we conclude that the three peaks in each group are due to clusters in different initial charge states with $\Delta Z=1$.

The presence of more than one initial charge state allows estimating the cluster size independently of the E_{∞} value, which is known with limited precision due to the uncertainty in the work function (3.95–4.25 eV for lead).^{25,26} In this context it is not even necessary to know exactly which peak corresponds to each charge state. The only requirement is that the cluster charge differences are one unit, so that the peak separation is equal to e^2/R . For the spectrum in Fig. 2(a) where the separation is equal to 0.71 eV we calculate a cluster radius of ≈ 20 Å, and the corresponding average size of $\langle N \rangle \approx 1 \times 10^3$ atoms or cluster mass $\langle M \rangle \approx 2 \times 10^5$ amu. The spectrum in Fig. 2(b) with ≈ 0.52 eV separation gave ≈ 28 Å cluster radius ($\langle N \rangle \approx 3 \times 10^3$ and $\langle M \rangle \approx 6 \times 10^5$ amu). Thus the method described above opens a way for cluster size estimation based on a simple analysis of core-level photoelectron spectra.

As a next step we can identify the initial charge states of the subcomponents in the spectra. For brevity we consider only the $5d_{5/2}$ spin-orbit related group. From recent work²⁷ the absolute value E_{∞} of the $5d_{5/2}$ state is found between the positions of the central peak and the lower energy subcomponent [Figs. 2(a) and 2(b)]. This automatically assigns the peaks in order of increasing binding energy as due to initially negative, neutral, and positive clusters. The results of our experiments with different magnetron powers (60–140 W) are in accord with this assignment: the relative intensity of the lower binding energy peak ($Z=-1$) increases with the magnetron power. High power leads to higher electron density in the plasma, and electron capture by clusters becomes more probable.

The experimentally determined values for E_{cl} and $\Delta E(Z,R)$ permit us to obtain an exact value for E_{∞} . Equation (1) gives $E_{\infty} = 22.0$ eV. As can be seen from Fig. 2(b) the neutral cluster peak shifts towards lower binding energy and approaches E_{∞} at larger cluster sizes. This shift is one more confirmation of the suggested assignment.

These core-level spectroscopy results shed additional light on the valence energy structure: the knowledge of $E_{\infty} = 22.0$ eV obtained in the present work allows us to derive the work-function value W_{∞} for the infinite bulk and for the different initial charge state clusters $W_{cl}(Z,R)$. From Refs. 25–27 the binding energy of the $5d_{5/2}$ level in solid lead relative to the Fermi level is equal to 18.0 eV. This results in a solid work function of 4.0 eV. The interval containing the work-function values for clusters of three different initial charge states is shown on the valence spectrum in Fig. 1. The center of the interval is placed at the position calculated for the initially neutral clusters with $\langle N \rangle \approx 3 \times 10^3$: $W_{cl} = W_{inf} + e^2/2R = 4.3$ eV. The width of the interval is equal to $2 \frac{e^2}{R}$. The initially charged clusters should contribute to the valence spectrum analogously to the core-level spectra. However, the valence cluster features are considerably broader than the core-level peaks. As a consequence the features arising from different charge states with $a \approx 0.5$ eV separation are not distinguishable in the valence spectrum (Fig. 1). This result, as well as all the results above, under-

line the unique possibilities of the core-level spectroscopy in the cluster research. Moreover, the ongoing activity focused on free metal clusters at a next-generation x-ray source—the free electron laser in Hamburg also confirms a large potential for core-level spectroscopy in this field.²⁹

Summarizing the results of the present work we conclude that XPS measurements on free metal clusters created by a magnetron-based gas aggregation source are feasible. We have demonstrated that the presence of metal clusters in different charge states resolved in XPS spectra provide direct

information on the cluster dimensions. For free large lead clusters we have determined core-level binding energies which approach infinite bulk values with the size. Both core-level and valence spectra demonstrate that we have studied free metallic nanoparticles.

We gratefully acknowledge the financial support of the Knut and Alice Wallenberg Foundation, the Swedish Foundation for Strategic Research, the Göran Gustafsson Foundation, and the Swedish Research Council.

*serguei.peredkov@sljus.lu.se

- ¹B. von Issendorff and O. Cheshnovsky, *Annu. Rev. Phys. Chem.* **56**, 549 (2005).
- ²G. Wertheim, *Phase Transitions* **24-26**, 203 (1990).
- ³O. Cheshnovsky, K. J. Taylor, J. Conceicao, and R. E. Smalley, *Phys. Rev. Lett.* **64**, 1785 (1990).
- ⁴S. L. Qiu, X. Pan, M. Strongin, and P. H. Citrin, *Phys. Rev. B* **36**, 1292 (1987).
- ⁵H. R. Siekmann, E. Holub-Krappe, Bu. Wrenger, Ch. Pettenkofer, and K. H. Meiwes-Broer, *Z. Phys. B: Condens. Matter* **90**, 201 (1993).
- ⁶O. Kostko, B. Huber, M. Moseler, and B. von Issendorff, *Phys. Rev. Lett.* **98**, 043401 (2007).
- ⁷S. Peredkov *et al.*, *Phys. Rev. B* **75**, 235407 (2007).
- ⁸M. Tchapyguine *et al.*, *J. Chem. Phys.* **120**, 345 (2004).
- ⁹O. Björneholm, F. Federmann, F. Fössing, and T. Möller, *Phys. Rev. Lett.* **74**, 3017 (1995).
- ¹⁰G. Öhrwall *et al.*, *Phys. Rev. Lett.* **93**, 173401 (2004).
- ¹¹G. Öhrwall *et al.*, *J. Chem. Phys.* **123**, 054310 (2005).
- ¹²T. Hatsui, H. Setoyama, N. Kosugi, B. Wassermann, I. L. Bradeanu, and E. Rühl, *J. Chem. Phys.* **123**, 154304 (2005).
- ¹³U. Zimmermann, N. Malinowski, U. Näher, S. Frank, and T. P. Martin, *Z. Phys. D: At., Mol. Clusters* **31**, 85 (1994).
- ¹⁴R. Karnbach, M. Joppien, J. Stapelfeldt, J. Wörmer, and T. Möller, *Rev. Sci. Instrum.* **56**, 1712 (1993).
- ¹⁵F. G. Amar, J. Smaby, and T. J. Preston, *J. Chem. Phys.* **122**, 244717 (2005).
- ¹⁶H. Haberland, M. Mall, M. Moseler, Y. Qiang, T. Reiners, and Y. Thurner, *J. Vac. Sci. Technol. A* **12**, 2925 (1994).
- ¹⁷H. Häkkinen, M. Moseler, O. Kostko, N. Morgner, M. A. Hoffmann, and B. v. Issendorff, *Phys. Rev. Lett.* **93**, 093401 (2004).
- ¹⁸M. Bässler *et al.*, *Nucl. Instrum. Methods Phys. Res. A* **469**, 382 (2001).
- ¹⁹M. Tchapyguine *et al.*, *Rev. Sci. Instrum.* **77**, 033106 (2006).
- ²⁰B. Vogt, B. Schmiedeskamp, and U. Heinmann, *Vacuum* **41**, 1118 (1990).
- ²¹S. Rondon and P. Sherwood, *Surf. Sci. Spectra* **5**, 83 (1998).
- ²²M. Tchapyguine *et al.*, *Europ. Phys. J. D* (to be published).
- ²³M. A. Hoffmann, G. Wrigge, and B. v. Issendorff, *Phys. Rev. B* **66**, 041404(R) (2002).
- ²⁴R. Morel, A. Brenac, P. Bayle-Guillemaud, C. Portemont, and F. L. Rizza, *Eur. Phys. J. D* **24**, 287 (2003).
- ²⁵G. M. Bancroft, W. Gudat, and D. E. Eastman, *J. Electron Spectrosc. Relat. Phenom.* **10**, 407 (1977).
- ²⁶K. Gürtler and K. Jacobi, *Surf. Sci.* **134**, 309 (1983).
- ²⁷J. Dalmas, H. Oughaddou, G. L. Lay, B. Aufray, G. Treglia, C. Girardeaux, J. Bernardini, J. Fujii, and G. Panaccione, *Surf. Sci.* **600**, 1227 (2006).
- ²⁸G. Makov and A. Nitzan, *J. Chem. Phys.* **88**, 5076 (2002).
- ²⁹M. Neeb (private communication).